ARTICLE
Journal of Cellular Biochemistry 116:2109–2119 (2015)

Journal of Cellular Biochemistry

Acute Treatment With XMetA Activates Hepatic Insulin Receptors and Lowers Blood Glucose in Normal Mice

Daniel H. Bedinger,[1,2] Dorothy A. Kieffer,[3] Ira D. Goldfine,[1] Marina K. Roell,[1] and Sean H. Adams[2,3,4*]

[1]*XOMA Corporation, Berkeley, California*

[2]*Molecular, Cellular and Integrative Physiology Graduate Group, University of California, Davis, California*

[3]*Graduate Group in Nutritional Biology -and- Department of Nutrition, University of California, Davis, California*

[4]*Arkansas Children's Nutrition Center -and- University of Arkansas for Medical Sciences, Department of Pediatrics, Little Rock, Arkansas*

ABSTRACT

It has been proposed that monoclonal antibodies may become therapeutics for metabolic diseases such as diabetes mellitus. We have previously characterized an allosteric monoclonal antibody to the human insulin receptor (IR), XMetA, that activated metabolic signaling leading to enhanced glucose transport in cultured cells, and chronically reduced fasting blood glucose levels in mouse models of diabetes mellitus. Under acute dosing conditions, the large size of an IR-binding antibody like XMetA (~150 kDa) could lead to a more rapid access into liver, an insulin sensitive tissue with well-fenestrated capillaries, when compared to other insulin sensitive tissues with non-fenestrated capillaries, such as muscle and adipose. Thus, in the present study we administered XMetA (10 mg/kg) and insulin (0.5 U/kg) via IV injection, and for 90 min compared their effects on blood glucose lowering and IR activation in three of the major insulin-sensitive tissues of the normal fasted mouse: liver, adipose, and muscle. Like insulin, XMetA lowered blood glucose levels, although the effect was less rapid. Insulin activated IR autophosphorylation and Akt phosphorylation in liver, fat, and muscle. In contrast, IR activation by XMetA was primarily observed in the liver. Both insulin and XMetA lowered β-hydroxybutyrate levels in plasma; however, only insulin reduced both non-esterified fatty acids (NEFA) and glycerol concentrations. These data indicate that, in normal mice, acute glucose regulation by XMetA is largely mediated by its action on the liver. J. Cell. Biochem. 116: 2109–2119, 2015. © 2015 Wiley Periodicals, Inc.

KEY WORDS: INSULIN RECEPTOR; INSULIN ANALOG; PARTIAL ALLOSTERIC AGONIST; CHO CELLS; LIVER; DIABETES

Insulin, via the insulin receptor (IR), lowers blood glucose through tissue-specific mechanisms. These mechanisms range from inhibiting hepatic glucose output (HGO) to stimulating the uptake of glucose into skeletal muscle and adipose tissues. It has been proposed that monoclonal antibodies to receptors may become novel therapeutics for treating diabetes mellitus [Ussar et al., 2011]. Recently we screened human phage display libraries and identified XMetA, an allosteric antibody to the human insulin receptor (hIR). Studies with cells expressing the hIR demonstrated that XMetA did not alter insulin binding or insulin action at the hIR [Bhaskar et al., 2012; Bedinger et al., 2015]. XMetA was a partial agonist of both hIR autophosphorylation and activation of the "metabolic" Akt pathway, and XMetA fully stimulated glucose uptake in cultured cells [Bhaskar et al., 2012].

XMetA was then studied in vivo both in insulinopenic mice [Bhaskar et al., 2012] and in insulin-resistant mice with diet-induced obesity (DIO) [Bhaskar et al., 2013]. In these models, XMetA treatment reduced fasting hyperglycemia for one month. These studies were consistent with the XMetA effects observed in cell culture studies, and demonstrated that XMetA acted in vivo to impact glucose homeostasis.

Insulin coupled to large molecules have previously been shown to preferentially activate hepatic insulin receptors [Shojaee-Moradie et al., 2000; Moore et al., 2014]. The liver sinusoids are highly

*Correspondence to: Sean H. Adams, Arkansas Children's Nutrition Center, 15 Children's Way, Little Rock, AR 72202. E-mail: shadams@uams.edu; former affiliation: Obesity & Metabolism Research Unit, Western Human Nutrition Research Center, United States Department of Agriculture-Agricultural Research Service (USDA-ARS)

Manuscript Received: 16 March 2015; Manuscript Accepted: 19 March 2015

Accepted manuscript online in Wiley Online Library (wileyonlinelibrary.com): 23 March 2015

DOI 10.1002/jcb.25168 • © 2015 Wiley Periodicals, Inc.

fenestrated compared to the capillaries of muscle and adipose tissue. Antibodies are large molecules (~150 kDa) and following acute treatment, antibody exposure to the liver is greater than in adipose or muscle [Vugmeyster et al., 2010]. Thus, it is possible that XMetA could primarily induce activation of hepatic IRs following acute administration. In order to further understand both the onset of the glucose-lowering actions and the relative activation by XMetA in different tissues when administered acutely, we injected normal mice intravenously (IV) with this antibody and evaluated its glucose-lowering efficacy in conjunction with determination of tissue-specific IR autophosphorylation and AKT phosphorylation.

Complementary studies considered the potential that patterns of tissue activation stem from differential activity of XMetA on IR splice variants. The mouse and human both express two IR splice variant isoforms: the 12 amino acids derived from exon 11 are included in the longer IR-B isoform, but not in the shorter IR-A isoform which lacks exon 11. The ratio of the two isoforms differs across insulin-responsive tissues [Moller et al., 1989; Goldstein and Dudley, 1990; Mosthaf et al., 1990; Sesti et al., 1994; Serrano et al., 2005]. Thus, we also evaluated the potency of XMetA to bind and stimulate cultured cells expressing either the mouse IR-A (mIR-A) or IR-B (mIR-B) isoform.

MATERIALS AND METHODS

STUDIES IN VIVO

All animal protocols were approved by the University of California at Davis Institutional Animal Care and Use Committee according to Animal Welfare Act guidelines.

The effect of acute intravenous treatment with XMetA on blood glucose levels in mice. Male C57BL/6J mice (10–12 weeks old, from The Jackson Laboratory, Bar Harbor, ME) were fed a chow diet (#2918, Harlan Teklad, Indianapolis, IN) on a 12 h light cycle. They were fasted for 5 h and then injected intravenously (IV), via the lateral tail vein, with either 10 mg/kg XMetA (XOMA, Berkeley, CA), 10 mg/kg control human monoclonal antibody (anti-keyhole limpet hemocyanin, XOMA), or 0.5 U/kg human insulin (Humulin R U-100, Eli Lilly, Indianapolis, IN). All compounds were diluted with injectable saline and injection volumes were between 25 and 35 μL. Blood glucose readings using a FreeStyle Lite glucometer (Abbott, Abbott Park, IL) were obtained by nicking the lateral tail vein with a sterile scalpel blade and gently milking a drop of blood from the tail. Each mouse was sampled at seven time points; immediately before injection, and at 10, 25, 60, 120, and 180 minutes after the injection. Mice were returned to their cages between samplings.

Tissue signaling effects of acute intravenous treatment with XMetA and insulin. Mice were fasted overnight. After 12–14 hours, the fasted mice were injected via the tail vein with one of the following: 10 mg/kg of either XMetA or control antibody, 0.5 U/kg human insulin (Humulin R U-100, Eli Lilly), or 10 U/kg human insulin (as a positive control for tissue protein phosphorylation analyses- 10 minute time point only), and returned to their cages. At 10, 25, or 90 min post-injection, sub-sets of mice were euthanized via CO_2 inhalation and the liver, epididymal white adipose tissue (EWAT), and whole gastrocnemius muscle were rapidly removed and snap frozen in liquid nitrogen. Blood was collected via cardiac puncture and then centrifuged to obtain EDTA-plasma, which was snap-frozen.

Evaluation of insulin signaling in liver, muscle and EWAT. Tissues were powdered while frozen using a liquid nitrogen-cooled Bessman tissue pulverizer (Spectrum Labs, Milpitas, CA). Lysates were made from an aliquot of the powdered tissue using ice-cold Tris lysis buffer (all lysis buffer components were from Sigma-Aldrich, St. Louis, MO, unless otherwise noted), 150 mM NaCl (Teknova, Hollister CA), 20 mM Trizma-HCl, pH 7.5, 1 mM EDTA, 1mM EGTA, 1% Triton X100, Phosphatase Inhibitors 2 and 3 (100 μL/10 mL), 2 mM PMSF, and 1X cOmplete protease inhibitor (Hoffman-La Roche, Basel Switzerland). Protein concentration was measured in lysates using the Bradford protein assay (Bio-Rad) and diluted with additional lysate buffer to equalize protein concentrations prior to loading on the gel. Samples were then analyzed by Western blot using antibodies recognizing total Akt, Akt phosphorylated at Thr^{308}, tubulin, and β-actin (antibodies from Cell Signaling, Danvers, MA). The antibody to IR phosphorylated at $Tyr^{1162/1163}$ was from EMD Millipore (Billerica, MA), and the antibody to IR phosphorylated at Tyr^{972} was from Invitrogen. Samples were reduced and run on a 10% Bis-Tris gel using MOPS-SDS (Life Technologies) running buffer and transferred to PVDF membranes using the TransBlot Turbo device (BioRad, Hercules, CA). Blots were blocked with Tris buffered saline with 0.1% Tween 20 and 5% bovine serum albumin (BSA), then probed with primary antibodies at a 1:5000 dilution. Detection was performed with anti-Rabbit IgG (H + L)-HRP (Jackson ImmunoResearch, West Grove, PA), imaged using SuperSignal West Dura Chemiluminescent Substrate (Pierce/ThermoFisher) and a ChemiDoc MP CCD imager (BioRad), quantitated with Image Lab software (BioRad), and normalized to the fold signal over control antibody treated mice for each marker.

Analysis of plasma samples. Plasma samples were analyzed for β-hydroxybutyrate using the Cayman Chemical Company colorimetric assay kit (#700190, Cayman Chemical, Ann Arbor, MI). Non-esterified fatty acids (NEFA) and glycerol were analyzed using the ZenBio Plasma Fatty Acid and Glycerol Kit (#GFA-1, Zen Bio, Research Triangle Park, NC). Plasma insulin was measured using an Ultra-Sensitive Mouse Insulin ELISA kit (#90080, Crystal Chem, Downers Grove, IL), with Humulin as the standard for insulin-treated animals. All assays were performed according to manufacturer's instructions.

CHO-MOUSE IR-A AND IR-B STUDIES

Establishment of cell lines. CHO-K1 cells were transfected with a stable plasmid containing the Neomycin resistance selection marker with cDNA sequences encoding either the mouse long form (mIR-B) or the short form (mIR-A; the 36 base pair exon 11 sequence deleted) of the IR [Yamaguchi et al., 1991; Bhaskar et al., 2012]. Cells were plated by limiting dilution in the presence of the G-418 (Life Technologies, Grand Island, NY) and cultured in Excel-302 media (Sigma-Aldrich, St. Louis, MO) to establish single clones. High-expressing cells were screened by flow cytometry for IR expression using the XMetA antibody and a goat anti-human IgG-Fc specific phycoerythrin-conjugated antibody (Jackson ImmunoResearch,

West Grove, PA). Both transfected cell lines had approximately 250,000 IR receptors per cell.

XMetA binding to either mouse IR-A or mouse IR-B expressing cells by flow cytometry. Cells were treated with various antibody concentrations at 4°C for 4 h. Cells were washed and incubated with a goat anti-human IgG-Fc specific phycoerythrin conjugated antibody (Jackson ImmunoResearch) and analyzed by flow cytometry. Assay buffer for the analysis was phosphate buffered saline (PBS) with 0.5% BSA and 0.1% sodium azide.

The effect of XMetA on insulin signaling in cultured cells. For studies evaluating the activation of insulin signaling events, CHO-K1 cells expressing the mouse IR-A or mouse IR-B isoform were incubated in DMEM (4 mM glucose, Life Technologies) with 0.3% BSA (Sigma Aldrich) for 5 h to reduce background signals, then incubated with increasing concentrations of either insulin or XMetA for 10 min. Cells were pelleted by centrifugation at 4°C, the supernatant was decanted, and the cells resuspended in cold Tris lysis buffer as above. Samples were analyzed by Western blot as above. Data were fit using GraphPad Prism™ software (sigmoidal dose-response, variable slope 4 parameter fit) to generate EC_{50} values.

Statistics. For all animal studies, there were 5–7 animals per group unless otherwise specified. Data are presented as the mean ± the SEM. Significance relative to the control antibody-treated condition was determined comparing differences in time-matched controls in using a Dunnett's multiple comparison test.

RESULTS

THE EFFECT OF INSULIN AND XMetA ON FASTING BLOOD GLUCOSE LEVELS

In normal male mice, the effect of IV XMetA on blood glucose levels was measured for up to 3 h, and compared to the effects of a control antibody and 0.5 U/kg insulin (Fig. 1). A submaximal insulin dose was selected in an attempt to match the partial agonist properties of XMetA, which even at high doses does not fully activate IR signaling in vitro [Bhaskar et al., 2012; Bedinger et al., 2015]. Fasting blood glucose levels were approximately 120 mg/dL. After 10 min, insulin at 0.5 U/kg lowered blood glucose levels to 80 mg/dL, with a nadir of ~60 mg/dL occurring at 60 min; glucose slightly increased at 120 and 180 min. Control antibody at 10 mg/kg elevated blood glucose levels at 10 and 25 min, an effect most likely due to the stress of the procedure. XMetA administration at 10 mg/kg also showed a similar transient increase in blood glucose levels at 10 min equivalent to that of the control antibody, but by 25 min a glucose-lowering effect of XMetA was apparent (blood glucose significantly lower than control antibody, $P < 0.05$). Blood glucose levels steadily decreased to a nadir of ~65 mg/dL at 120 min and remained at this level at 180 min. Thus, both the 0.5 U/kg insulin treatment and the 10 mg/kg XMetA treatment elicited similar maximal reductions in blood glucose levels, although the time course for the two agents were different.

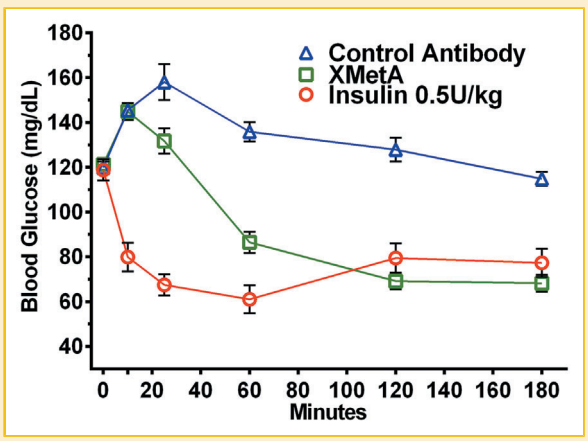

Fig. 1. Blood glucose responses following the acute IV administration of either Control Antibody, XMetA or insulin to adult male mice. C57BL/6J mice were fasted 5 h and then dosed IV with 10 mg/kg XMetA (square), 10 mg/kg negative control antibody (triangle), or 0.5 U/kg human insulin (circle). Values are the mean ± SEM, n = 8 per group.

THE EFFECT OF INSULIN AND XMetA ON INSULIN RECEPTOR SIGNALING IN TISSUES

Since both low-dose insulin and XMetA reduced blood glucose levels to an equivalent degree in normal fasted mice, we studied the effect of these agents on the three major insulin-responsive tissues: liver, adipose, and skeletal muscle (gastrocnemius). We analyzed phosphorylation of the IR and Akt in these tissues at 10, 25 and 90 min after administration.

Insulin levels. Ten minutes after injection, plasma insulin levels in both the control mice and XMetA-treated mice were relatively low at 330 ± 87 pg/mL and 172 ± 33 pg/mL respectively (Fig. 2A), and remained low for the duration of the study, whereas plasma insulin levels exceeded 400 ng/mL in the high dose insulin group and were 12.5 ± 1.0 ng/mL in the 0.5 U/kg insulin group. At 25 min after injection, the insulin levels in the 0.5 U/kg group had fallen to 6.3 ± 1.0 ng/mL. At 90 min, insulin levels in all groups were similar.

Liver. When IR autophosphorylation at tyrosine 972 ($pTyr^{972}$) was measured in liver (Fig. 2C), the 10 U/kg positive control insulin treatment induced a nearly 25-fold increase over control mice at 10 min (no further time points were tested for the high-dose insulin treated mice since these animals would have become severely hypoglycemic). At this time point both the 0.5 U/kg insulin and the XMetA doses induced a 2.5–3.5-fold increase in $pTyr^{972}$ over control. At 25 min, the effect of 0.5 U/kg insulin was decreased from that seen at 10 min, whereas the effect of XMetA had increased to approximately fivefold over control. At 90 min the insulin response had returned to baseline, but the effect of XMetA remained similar to the 25 min time point. When IR autophosphorylation at the kinase regulatory loop tyrosines 1162/1163 ($pTyr^{1162/1163}$) was measured (Fig. 2D), a similar pattern was seen. At 10 min, high dose insulin stimulated a ninefold increase in autophosphorylation. Both the 0.5 U/kg insulin and XMetA groups showed an elevated phosphotyrosine level over the control (1.5- and 2-fold, respectively, $P < 0.05$). By 25 min, the response to insulin was similar to that of control, but the XMetA-induced $pTyr^{1162/1163}$ levels were markedly higher and by 90 min had risen to nearly fourfold that of the control group. These results indicated that both insulin and XMetA robustly

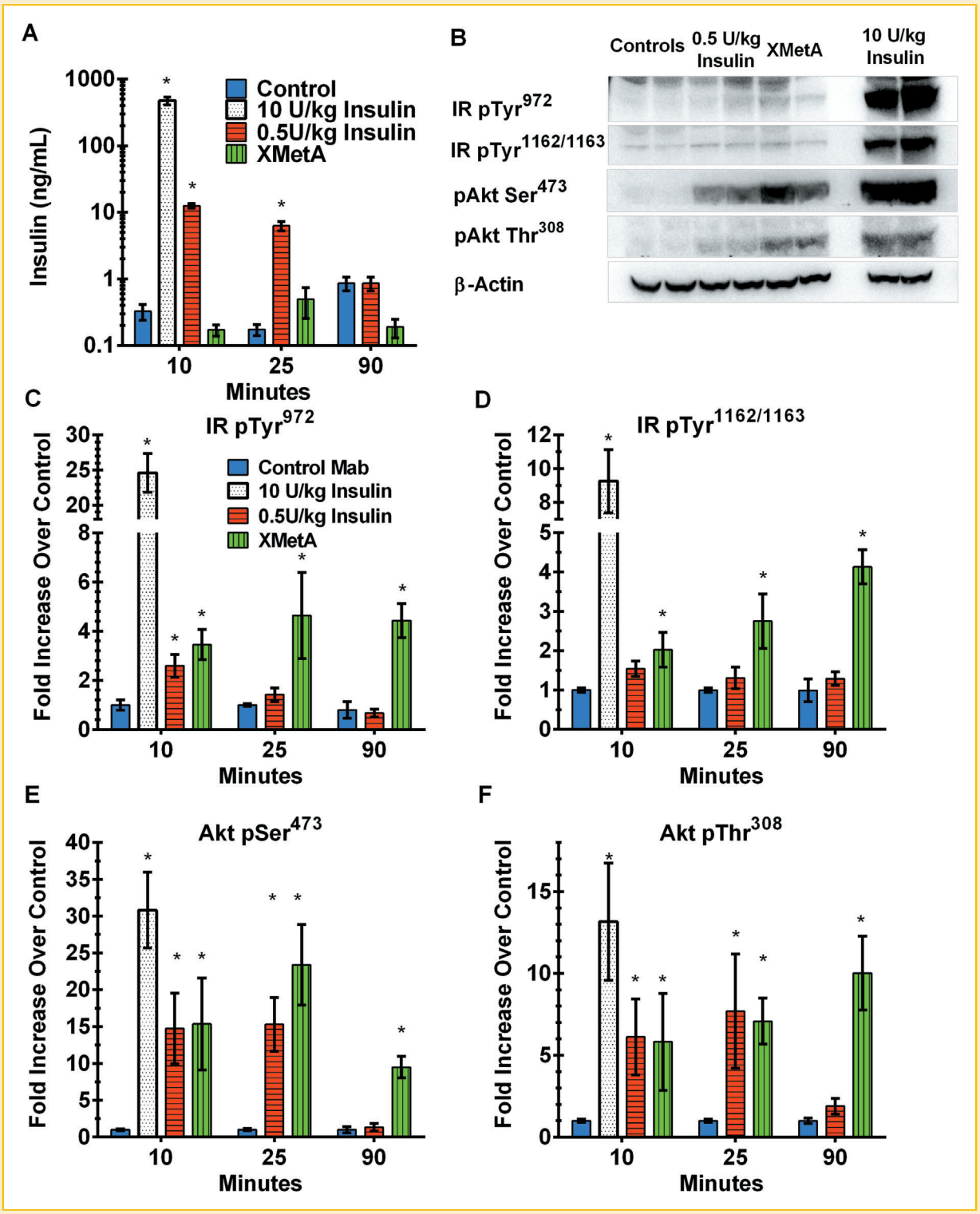

Fig. 2. Insulin receptor signaling in the liver of adult male mice dosed with IV insulin or XMetA. Mice were fasted and then dosed IV with either 10 mg/kg negative control antibody (blue), 10 U/kg positive control insulin (white), 0.5 U/kg insulin (red), or 10 mg/kg XMetA (green). Plasma insulin levels were measured by ELISA (A). Western blots from two representative mice from each treatment group at 10 min are shown for illustration (B). Liver tissues were removed at specified times and analyzed by Western blots for IR phosphorylation at Tyr^{972} (C), $Tyr^{1162/1163}$ (D); and for Akt phosphorylation at Ser^{473} (E) and Thr^{308} (F). $^{*}P < 0.05$ versus control antibody within time point. Values are the mean ± SEM. N = 5–7 per animals per group.

stimulated hepatic insulin receptor autophosphorylation. However, the time course of this activation differed for the two agents as the effect of XMetA was more durable.

Next, we evaluated the effects of insulin and XMetA administration on the activation of Akt, a key kinase involved in metabolic signaling by the activated IR [Taniguchi et al., 2006]. Two regulatory phosphorylation sites on Akt were evaluated, threonine 308 (Thr^{308}) and serine 473 (Ser^{473}) (Fig. 2E and F). These phosphorylation sites on Akt showed similar responses to both agents. After 10 minutes, both insulin treatments and XMetA treatment induced large increases in Akt phosphorylation. At this time point high dose insulin induced 30- and 13-fold increases in Ser^{473} and Thr^{308} phosphorylation respectively. Low dose insulin and XMetA induced 15- and 5-fold increases, respectively at this time point. At 25 min, low dose insulin and XMetA responses were also similar. At 90 min, the insulin-treated mice had returned to baseline levels of Akt phosphorylation, while the XMetA response persisted. In XMetA-treated mice, Ser^{473} showed peak levels of phosphorylation at 25 min and a modest reduction by 90 min, whereas the Thr^{308} site showed similar responses at 25 and 90 min.

White adipose tissue (WAT). At 10 min, the high dose insulin caused a 20-fold increase in $pTyr^{972}$ and $pTyr^{1162/1163}$ autophosphorylation sites in EWAT (Fig. 3A and B). In response to 0.5 U/kg insulin, a more modest activation of these IR autophosphorylation sites, sixfold or less, was evident at 10 min and persisted above baseline levels at 25 and 90 min. In contrast, XMetA did not induce IR autophosphorylation in EWAT at either site at any time point. Akt phosphorylation responses in EWAT were consistent with the pIR responses (Fig. 3C and D) with insulin inducing clear responses at 10 and 25 min for both Akt phosphorylation sites, while XMetA treatment did not result in Akt phosphorylation in EWAT at either site at any time point.

Skeletal muscle. At 10 min, the high dose of insulin induced a 25- and 8-fold increase in the $pTry^{972}$ and $pTyr^{1162/1163}$ autophosphorylation sites, respectively (Fig. 4A and B). In response to 0.5 U/kg insulin, more modest activation of these insulin receptor autophosphorylation sites (fivefold or less) was evident at 10 min, but was equivalent to control levels at 25 and 90 min. In muscle, like in EWAT, XMetA did not induce IR autophosphorylation at either site, at any time point. In muscle, Akt phosphorylation (Fig. 4C and D) by the 0.5 U/kg insulin dose group was more durable than the pIR response as insulin-induced Akt phosphorylation was evident at both 10 and 25 min for both Akt phosphorylation sites, but had diminished by 90 min. XMetA treatment did not result in Akt phosphorylation in muscle at either site at any time point.

THE EFFECT OF INSULIN AND XMetA ON PLASMA MARKERS REFLECTIVE OF INSULIN ACTION AT LIVER AND ADIPOSE

To provide insight into potential tissue-specific metabolic effects, complementary to tissue protein phosphorylation patterns, plasma metabolites that are responsive to insulin action at the liver and in white adipose tissue were measured. The liver produces ketone bodies during fasting, a function that is inhibited by activation of the IR [McGarry and Foster, 1980]. Both the high and low doses of insulin caused a large and immediate reduction in β-hydroxybutyrate (β-HB) concentration by the 10 min time point, dropping from 1.1 mM to 0.4 mM, and this reduction in β-HB persisted at 25 and 90 min, when compared to the control ($P = 0.0001$ and $P = 0.007$, respectively) (Fig. 5A). XMetA treatment also lowered β-HB levels at all the time points, being statistically significant at 90 min ($P = 0.23$, $P = 0.09$, and $P = 0.002$ versus control at 10, 25, and 90 min, respectively).

Plasma NEFA and glycerol concentrations were also evaluated (Fig. 5B and C). The 0.5 U/kg insulin treatment elicited a significant reduction in NEFA levels compared to the control antibody at all time points ($P < 0.005$ for all). XMetA-treated mice showed no significant reduction of NEFA at 10 or 90 min, but did show a significant reduction in NEFA at 25 min ($P = 0.004$). Glycerol levels were qualitatively similar to NEFA, and 0.5 U/kg insulin showed lower mean glycerol levels at 25 and 90 min versus control, but differences were not statistical significant by ANOVA. XMetA-treated group glycerol values, as with NEFA, also showed somewhat lower mean than control at 25 minutes, but were at no time were statistically different from controls.

STUDIES IN VITRO

Binding and IR activation by XMetA in CHO cells expressing either the mouse IR-A or IR-B receptor isoforms. Liver, muscle, and adipose tissue have different ratios of the two IR isoforms [Moller et al., 1989; Goldstein and Dudley, 1990; Mosthaf et al., 1990; Sesti et al., 1994; Serrano et al., 2005]. In murine tissues, the liver predominately expresses isoform B, whereas muscle tissue expresses predominately the A isoform of IR, and adipose tissue expresses both IR isoforms at similar levels [Serrano et al., 2005]. To rule out that the tissue-specific effects of acutely-dosed XMetA observed in vivo were due to differential binding of the antibody to the mIR-A versus mIR-B receptor isoforms, we tested binding characteristics of XMetA to these isoforms in CHO-K1 cells expressing either mIR-A or mIR-B. XMetA bound to both the mIR-A and mIR-B cell lines with similar dose responses (EC_{50} 708 ± 50 pM for mIR-A and 568 ± 86 pM for mIR-B) (Fig.6). XMetA binding was not influenced by either the presence or absence of saturating concentrations of insulin.

The cells expressing either mIR-A or mIR-B were stimulated with various concentrations of either insulin or XMetA. Then IR autophosphorylation was analyzed at the β-subunit tyrosine kinase regulatory loop domains ($pTyr^{1150/1151}$ or $pTyr^{1162/1163}$) (Fig. 7). In both cell lines, XMetA was a partial agonist of IR activation and autophosphorylation, with nearly identical levels of IR autophosphorylation (20% that of insulin). Moreover, the dose responses for XMetA were very similar (EC_{50} values 9.2 ± 1.7 nM for the mIR-A and 8.1 ± 1.8 nM for the mIR-B). These results indicated that XMetA had a very similar ability to activate the mouse IR-A and mouse IR-B isoforms.

DISCUSSION

Our previous studies with XMetA, an allosteric IR partial agonist antibody [Bhaskar et al., 2012; Bhaskar et al., 2013], demonstrated marked improvements in fasting blood glucose levels in both diabetic and insulin-resistant mice that were chronically treated. In those studies it was unknown which tissues participated in the acute

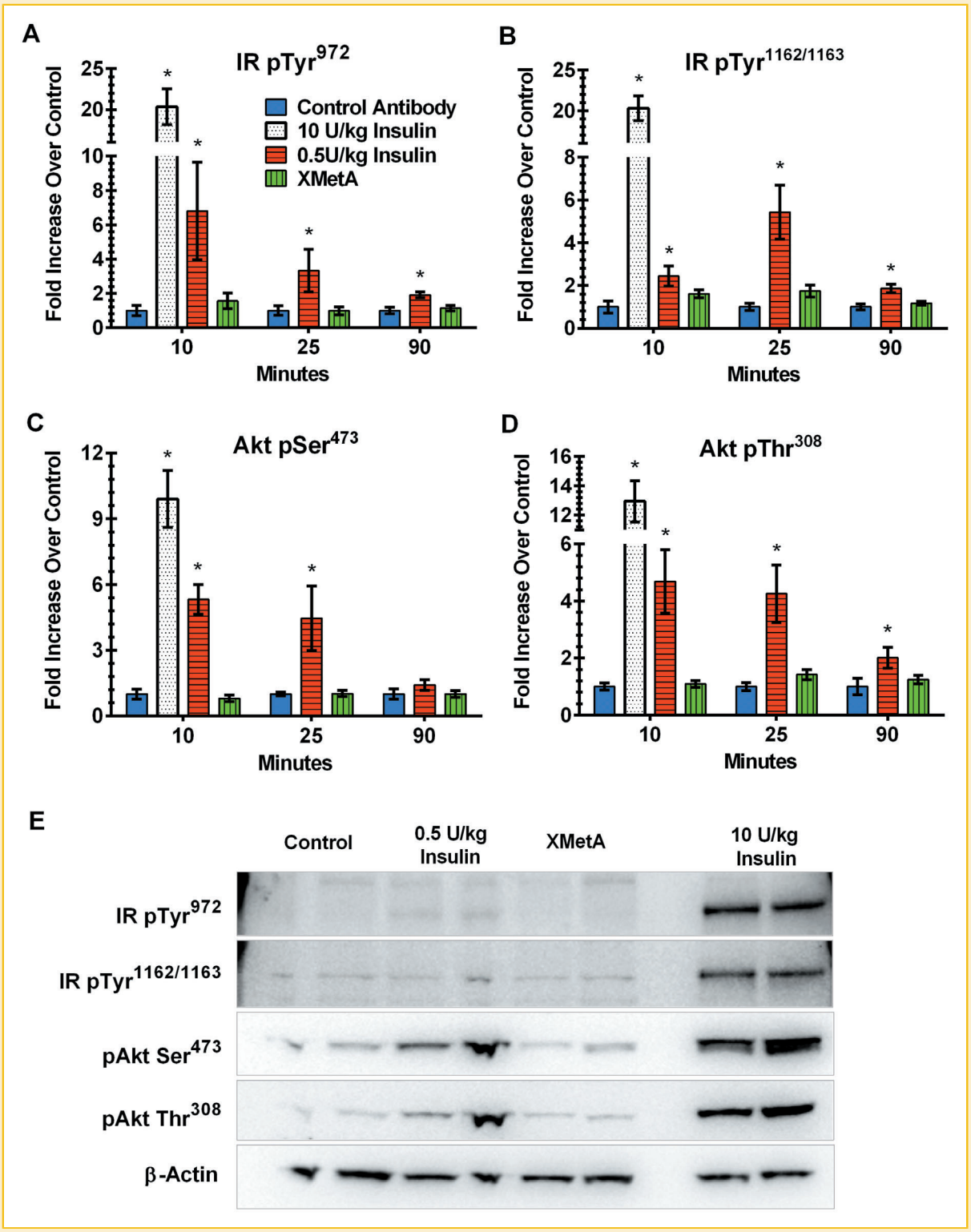

Fig. 3. Insulin receptor signaling in epididymal white adipose tissue of adult male mice administered insulin or XMetA. Mice were fasted and then dosed IV with either 10 mg/kg negative control antibody (blue), 10 U/kg positive control insulin (white), 0.5 U/kg human insulin (red), or 10 mg/kg XMetA (green). Tissues were removed at specified times and analyzed by Western blots for insulin receptor phosphorylation at Tyr^{972} (A), $Tyr^{1162/1163}$ (B), and for Akt phosphorylation at Ser^{473} (C) and Thr^{308} (D). $^{*}P < 0.05$ versus control antibody within time point. Values are the mean ± SEM. n = 5–7 per animals per group. Western blots from two representative mice from each treatment group at 10 min are shown for illustration (E).

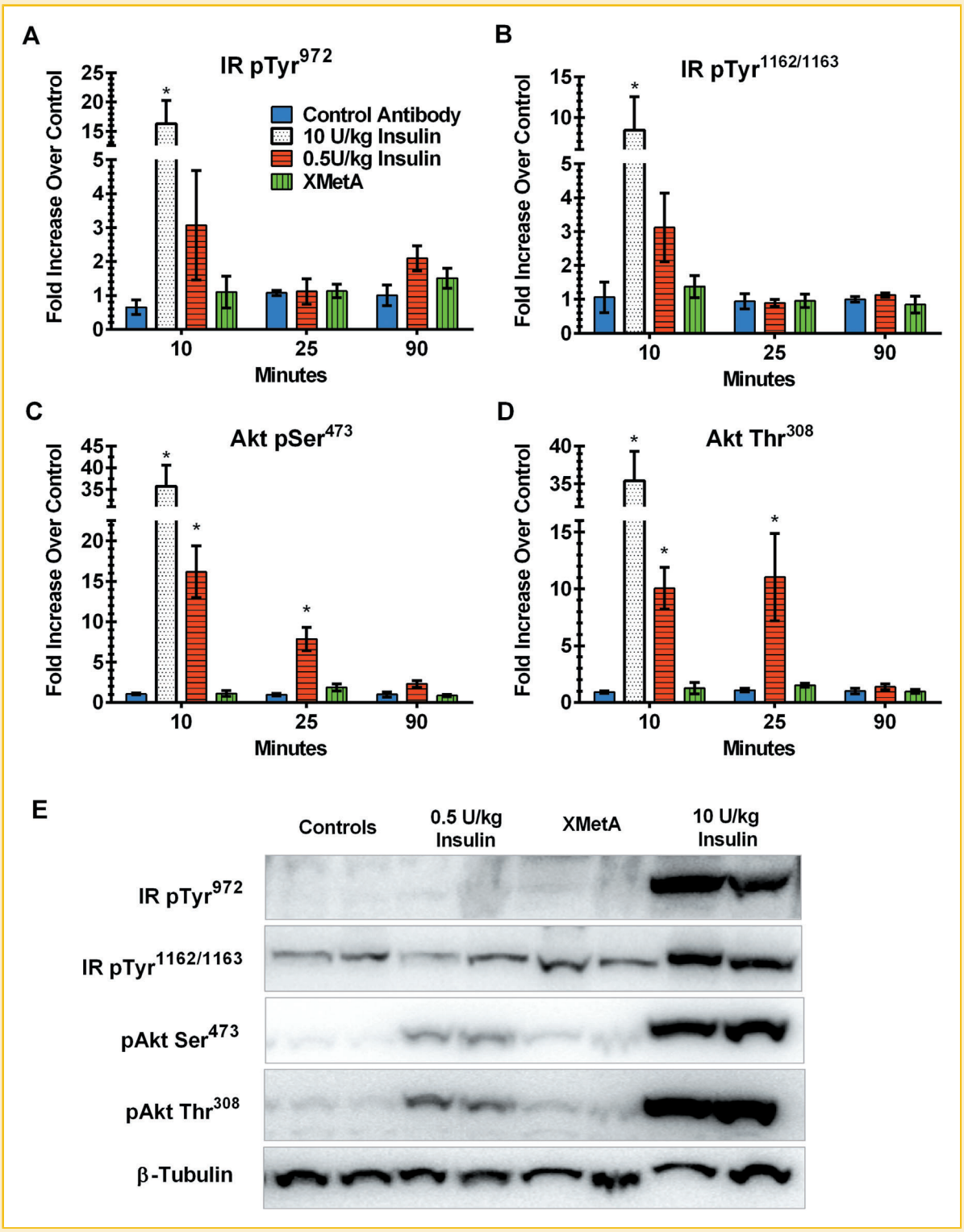

Fig. 4. Insulin receptor signaling in muscle tissue of adult male mice dosed with insulin or XMetA. Mice were fasted and then dosed IV with either 10 mg/kg negative control antibody (blue), 10 U/kg positive control insulin (white), 0.5 U/kg human insulin (red), or 10 mg/kg XMetA (green). Tissues were removed at specified times and analyzed by Western blots for insulin receptor phosphorylation at Tyr^{972} (A), $Tyr^{1162/1163}$ (B), and for Akt phosphorylation at Ser^{473} (C) and Thr^{308} (D). $^{*}P < 0.05$ versus control antibody within time point. Values are the mean ± SEM. n = 5–7 per animals per group. Western blots from two representative mice from each treatment group at 10 min are shown for illustration (E).

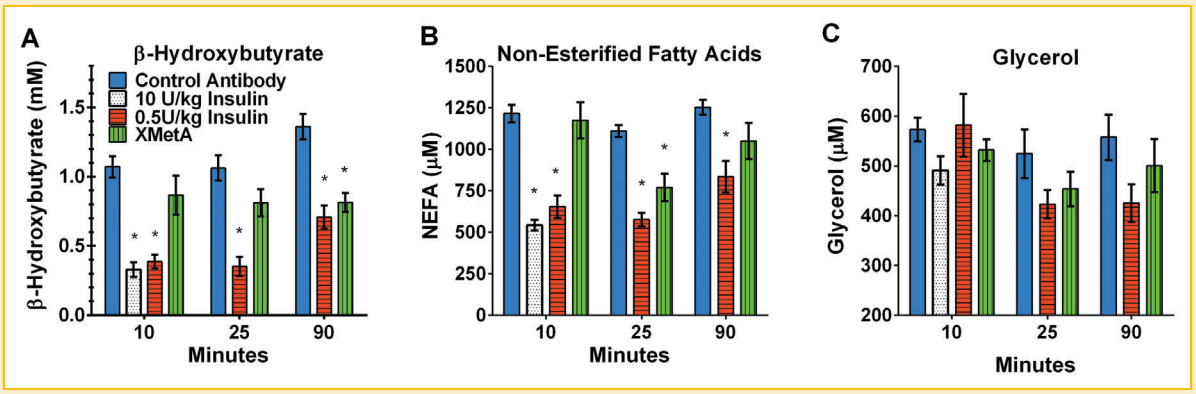

Fig. 5. Insulin and XMetA effects on plasma ketone body and lipolysis parameters. Plasma from treated mice were analyzed for β-hydroxybutyrate (A), non-esterified fatty acids (NEFA) (B), and glycerol (C) by colorimetric assays. $^{*}P < 0.05$ versus negative control antibody within time point. Values are the mean ± SEM. n = 5–7 per animals per group.

glucose-lowering effects of XMetA. Since antibodies are much larger in size when compared to peptide hormones such as insulin, it is likely that after acute exposure, tissues with a highly fenestrated endothelium such as liver would be initially targeted by XMetA. Therefore, in the current study we focused on the acute metabolic effects of XMetA, in order to determine whether the liver is a primary site of action of this antibody on insulin signaling parameters.

Intravenous XMetA administration decreased fasting blood glucose levels in normal mice 25–60 min after injection, and these reductions persisted for the duration of the experiment (180 min). An important finding was that XMetA rapidly activated IR autophosphorylation and Akt phosphorylation in the liver, but unlike insulin, XMetA did not activate IR signaling pathways in skeletal muscle and adipose tissue within 90 min. This acute action of XMetA on the liver was adequate to lower blood glucose levels equivalent to those observed with the acute IV administration of 0.5 U/kg insulin. These observations suggested that in normal mice acute IV administration of XMetA, for at least the first 90 min, activated hepatic IRs, and that the XMetA-stimulated reductions in blood glucose most likely reflect a reduction in hepatic glucose output (HGO) rather than increased peripheral glucose uptake [Camu, 1975]. Thus, our data indicate that the acute glucose-lowering effects of insulin and XMetA are mediated by different sets of tissue responses. However, monoclonal antibodies do eventually get distributed to peripheral tissues following IV dosing, with extra-cellular fluid concentrations equilibrating within 48 h [Lobo et al., 2004; Wang et al., 2008; Vugmeyster et al., 2010]. Thus, as XMetA gets distributed to the peripheral tissues, it is probable that activation of IR signaling in the muscle and adipose tissue by XMetA would also contribute to its glucose-lowering effects.

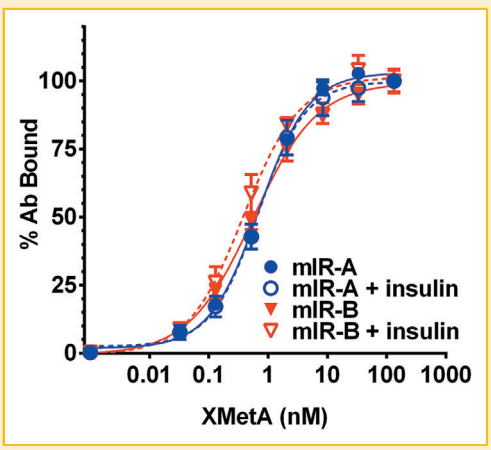

Fig. 6. XMetA binding to mouse IR-A or mouse IR-B. Binding of the XMetA antibody to CHO cells expressing either the mouse IR-A (triangles) or the mouse IR-B isoform (circles) was analyzed by flow cytometry. Binding analysis was performed in the presence (open markers) or absence (solid markers) of 175 nM insulin. Values are the mean of three independent determinations ± SEM.

In addition to the direct measurement of the molecular activation of insulin signaling pathways in the tissues, the measurements of plasma levels of β-HB, NEFA, and glycerol were generally consistent with the hypothesis that the acute effects of XMetA were primarily manifested in the liver. During fasting, the body normally shifts toward fat metabolism [Cahill, 2006; Keller et al., 1977; McGarry, 1992], and fatty acids and glycerol are released by lipolysis in adipose tissue. Then β -oxidation of fatty acids in the liver results in the production of the "ketone bodies", β-HB and acetoacetate. β-HB is the most abundant ketone body and is exported to the serum where it can be utilized by critical organ systems such as the heart and brain as an alternate fuel source [Owen et al., 1967; Stanley et al., 2005]. This process is negatively regulated by insulin [McGarry and Foster, 1980; Bluher et al., 2004]. The reduction in ketone levels following insulin treatment is a combined result of both insulin′s direct actions on the liver to inhibit hepatic fatty acid oxidation and ketogenesis, as well as the insulin′s inhibition of lipolysis in adipose tissue which reduces the availability of fatty acids to act as fuel for hepatic β-oxidation and ketone production [Randle et al., 1965; McGarry, 1992; Zammit, 1996]. Blood NEFA is strongly influenced by lipolysis in adipose tissue, and in the present study, as expected, insulin at 0.5 U/kg, rapidly and persistently reduced its concentrations. In comparison to insulin, changes in NEFA and glycerol

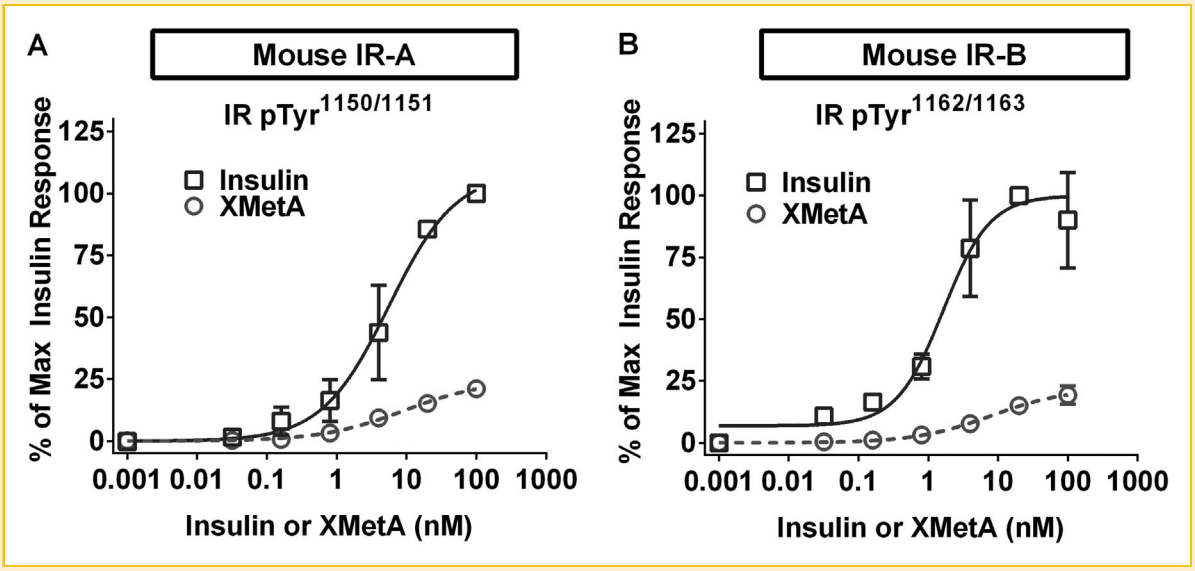

Fig. 7. Insulin and XMetA have similar activation of mIR-A and mIR-B expressed in CHO-K1 cells. CHO-K1 cells expressing either the mIR-A (A) or the mIR-B (B) isoform were incubated for 10 min with various concentrations of either insulin or XMetA. Cells were lysed and then analyzed by Western blot for phosphorylation of the mIR β-subunit tyrosine kinase regulatory loop domain ($pTyr^{1150/1151}$ or $pTyr^{1162/1163}$). Values are the mean of three independent determinations ± SEM.

were negligible following XMetA treatment. However, XMetA administrations significantly decreased β-HB in mice at 90 min, suggestive of metabolic effects in liver [Zammit, 1996], which is consistent with IR and Akt phosphorylation patterns.

We also investigated whether the tissue activation patterns of acutely-dosed XMetA was related to a differential activation of IR receptor isoforms, since the relative abundances of IR-A and IR-B differ across insulin-responsive tissues [Moller et al., 1989; Goldstein and Dudley, 1990; Mosthaf et al., 1990; Sesti et al., 1994; Serrano et al., 2005]. XMetA has previously been shown to bind and activate the human IR-A and IR-B forms equivalently [Bedinger et al., 2015], but it was not known whether the murine IR isoforms behaved in a similar manner. The current study confirmed a lack of isoform specificity for the mouse IR. This analysis also recapitulated, on both isoforms of the mouse IR, the allosteric and partial agonist properties of XMetA previously reported for the human IR [Bhaskar et al., 2012; Bedinger et al., 2015]. XMetA can bind to and activate both isoforms of the mouse IR equally; thus, any differential tissue effects observed in the present study were not a result of IR isoform selectivity.

A potential explanation for the predominant action in liver by acutely-dosed XMetA is the large size of the XMetA molecule, which is ~150 kDa. This size would be expected to slow the distribution to tissues such as WAT and muscle compared to the well-fenestrated environment of the liver. Consistent with this view, a pegylated form of the insulin analog lispro, LY2605541, which has mass of roughly 26 kDa, but a hydrodynamic radius equivalent to a much larger globular protein (~80 kDa) [Madsbad, 2014], has been shown to have a dominant action on the liver [Madsbad, 2014; Moore et al., 2014]. Another insulin-conjugate bound to thyroid hormone binding proteins (THBPs) was also "hepato-selective"[Shojaee-Moradie et al., 2000]. The proposed mechanism for the preferentially hepatic action of both molecules is their large molecular size and slow kinetics of distribution through the non-fenestrated endothelium of WAT and muscle [Shojaee-Moradie et al., 2000; Madsbad, 2014; Moore et al., 2014]. This mechanism suggests that large molecule insulin receptor agonists could have a tendency for hepatic action, at least under acute dosing conditions. The idea of tissue access regulating insulin action has been demonstrated in studies where the timing of appearance of insulin in muscle lymph coincided with the timing of insulin IR kinase activation and tissue glucose disposal [Miles et al., 1995]. Studies have shown that antibodies can be relatively slow to move out of capillaries with intact endothelial tight junctions and must be actively transported into tissues [Garg and Balthasar, 2007; Vugmeyster et al., 2010; Yip et al., 2014]. A large study using radio-labelled antibodies by Vugmeyster et al. found that at 1 hour post-IV dose, antibody exposure was an order of magnitude higher in the liver than in fat and muscle [Vugmeyster et al., 2010]. This observation could explain why the acute glucose lowering of XMetA is primarily associated with metabolic actions in the liver. Future studies will be needed to determine whether more chronic exposure to XMetA will activate the IR in non-hepatic tissues.

It is interesting to consider whether predominantly hepatic activation by an IR agonist would be useful clinically. The pancreas secretes insulin into the hepatic portal circulation and the liver is exposed to much higher insulin concentrations than the periphery due to both dilution of portal blood and the removal of roughly half of the secreted insulin by the liver [Chap et al., 1987]. This process results in the liver cells receiving a greater exposure to insulin than the peripheral tissues under normal physiological conditions [Camu, 1975; Chap et al., 1987]. In contrast, treatment of insulin-dependent diabetes patients involves insulin injected subcutaneously, and the liver is exposed to this exogenous insulin at the same level as the

periphery. The relative contribution of elevated portal insulin on glucose homeostasis has been the subject of some debate [Mittelman et al., 1997; Cherrington et al., 1998; Steil et al., 1998] and techniques to measure the regulation of hepatic insulin action are complicated by the intricate relationship between insulin and glucagon in the various experimental systems [Mittelman et al., 1997; Cherrington et al., 1998; Steil et al., 1998; Unger and Cherrington, 2012]. However, in normal mice, direct hepatic insulin action is an important contributor to glucose homeostasis and the differences in insulin exposure resulting from peripheral insulin therapy shift the balance of insulin action away from the liver toward muscle and adipose tissues [Cherrington et al., 1998; Sindelar et al., 1998]. It is possible that insulin therapies with preferential hepatic activation would, in some ways, better mimic the higher liver insulin exposure observed under physiological conditions.

In terms of the sensitivity of the response, low dose IV insulin is more effective at reducing hepatic glucose production relative to the stimulation of glucose uptake in muscle [Brown et al., 1978; Rizza et al., 1981]. The reduced HGO from low dose insulin is a combined effect of direct hepatic insulin action and a reduction of lipolysis in adipose tissue, as the beta-oxidation of NEFA are a key mechanism of maintaining blood glucose during fasting and hypoglycemia, both in terms of supporting HGO and glucose-sparing metabolic changes [Randle et al., 1965; Brown et al., 1978; Fanelli et al., 1993]. The systemically-elevated insulin levels resulting from peripheral insulin therapy acts on the muscle and adipose tissue to both increase glucose uptake and decrease the availability of gluconeogenic substrates coming to the liver [Sindelar et al., 1996]. In insulin-dependent patients, this dual mechanism of reducing blood glucose can potentially limit the effectiveness of the counter-regulatory response and increase the likelihood of hypoglycemic events [Moore et al., 2014]. Therefore, a drug that could reduce HGO by acting primarily on the liver has the potential to be both efficacious at reducing fasting and inter-meal blood sugars, but would carry less risk of hypoglycemia due to an inability to prevent the release of alternate metabolic fuel sources from adipose and muscle tissues [Moore et al., 2014]. Despite the high dose of XMetA given in this study, none of the mice became dangerously hypoglycemic, similar to prior studies administering XMetA to rodent models of insulin resistance and/or diabetes [Bhaskar et al., 2012; Bhaskar et al., 2013]. Therefore this profile of potent activation of liver IR signaling and durable action without severe hypoglycemia may be therapeutically valuable if these effects are recapitulated in humans. Further long and short term studies in higher species will be needed to better understand the therapeutic effect of XMetA.

ACKNOWLEDGMENTS

This work was funded by a Cooperative Research and Development Agreement (CRADA 58-3K95-1-1497) between XOMA Corp. and USDA-ARS, as well as through USDA-ARS intramural Project 5306-51530-019-00D (S.H.A.). USDA-ARS is an equal opportunity provider and employer. We would like to thank Kikumi Ono-Moore for assistance with the study, Fawaz Haj and Ahmed Bettaieb (University of California, Davis) for assistance with protocols.

CONFLICT OF INTERESTS

DH Bedinger, ID Goldfine, and MK Roell are employees of XOMA (US) LLC. There are no other conflicts of interest to report.

AUTHOR CONTRIBUTIONS

DH Bedinger, MK Roell, and SH Adams designed the experiments, DH Bedinger implemented the studies, conducted analyses, and wrote the manuscript. DA Kieffer assisted with the experimental work and the development of protocols. ID Goldfine, MK Roell, and SH Adams assisted with the interpretation of data and writing of the manuscript.

REFERENCES

Bedinger DH, Goldfine ID, Corbin JA, Roell MK, Adams SH. 2015. Differential pathway coupling of the activated insulin receptor drives signaling selectivity by XMetA, an allosteric partial agonist antibody. J Pharmacol Exp Ther. 353(1):35–43.

Bhaskar V, Goldfine ID, Bedinger DH, Lau A, Kuan HF, Gross LM, Handa M, Maddux BA, Watson SR, Zhu S, Narasimha AJ, Levy R, Webster L, Wijesuriya SD, Liu N, Wu X, Chemla-Vogel D, Tran C, Lee SR, Wong S, Wilcock D, White ML, Corbin JA. 2012. A fully human, allosteric monoclonal antibody that activates the insulin receptor and improves glycemic control. Diabetes 61:1263–1271.

Bhaskar V, Lau A, Goldfine ID, Narasimha AJ, Gross LM, Wong S, Cheung B, White ML, Corbin JA. 2013. XMetA, an allosteric monoclonal antibody to the insulin receptor, improves glycaemic control in mice with diet-induced obesity. Diabetes Obes Metab 15:272–275.

Bluher M, Patti ME, Gesta S, Kahn BB, Kahn CR. 2004. Intrinsic heterogeneity in adipose tissue of fat-specific insulin receptor knock-out mice is associated with differences in patterns of gene expression. J Biol Chem 279: 31891–31901.

Brown PM, Tompkins CV, Juul S, Sonksen PH. 1978. Mechanism of action of insulin in diabetic patients: A dose-related effect on glucose production and utilisation. Br Med J 1:1239–1242.

Cahill GF, Jr. 2006. Fuel metabolism in starvation. Annu Rev Nutr 26:1–22.

Camu F. 1975. Hepatic balances of glucose and insulin in response to physiological increments of endogenous insulin during glucose infusions in dogs. Eur J Clin Invest 5:101–108.

Chap Z, Ishida T, Chou J, Hartley CJ, Entman ML, Brandenburg D, Jones RH, Field JB. 1987. First-pass hepatic extraction and metabolic effects of insulin and insulin analogues. Am J Physiol 252:E209–217.

Cherrington AD, Edgerton D, Sindelar DK. 1998. The direct and indirect effects of insulin on hepatic glucose production in vivo. Diabetologia 41:987–996.

Fanelli C, Calderone S, Epifano L, De Vincenzo A, Modarelli F, Pampanelli S, Perriello G, De Feo P, Brunetti P, Gerich JE, et al. 1993. Demonstration of a critical role for free fatty acids in mediating counterregulatory stimulation of gluconeogenesis and suppression of glucose utilization in humans. J Clin Invest 92:1617–1622.

Garg A, Balthasar JP. 2007. Physiologically-based pharmacokinetic (PBPK) model to predict IgG tissue kinetics in wild-type and FcRn-knockout mice. J Pharmacokinet Pharmacodyn 34:687–709.

Goldstein BJ, Dudley AL. 1990. The rat insulin receptor: Primary structure and conservation of tissue-specific alternative messenger RNA splicing. Mol Endocrinol 4:235–244.

Keller U, Chiasson JL, Liljenquist JE, Cherrington AD, Jennings AS, Crofford OS. 1977. The roles of insulin, glucagon, and free fatty acids in the regulation of ketogenesis in dogs. Diabetes 26:1040–1051.

Lobo ED, Hansen RJ, Balthasar JP. 2004. Antibody pharmacokinetics and pharmacodynamics. J Pharm Sci 93:2645–2668.

Madsbad S. 2014. LY2605541-A preferential hepato-specific insulin analogue. Diabetes 63:390–392.

McGarry JD. 1992. What if Minkowski had been ageusic? An alternative angle on diabetes. Science 258:766–770.

McGarry JD, Foster DW. 1980. Regulation of hepatic fatty acid oxidation and ketone body production. Annu Rev Biochem 49:395–420.

Miles PD, Levisetti M, Reichart D, Khoursheed M, Moossa AR, Olefsky JM. 1995. Kinetics of insulin action in vivo. Identification of rate-limiting steps. Diabetes 44:947–953.

Mittelman SD, Fu YY, Rebrin K, Steil G, Bergman RN. 1997. Indirect effect of insulin to suppress endogenous glucose production is dominant, even with hyperglucagonemia. J Clin Invest 100:3121–3130.

Moller DE, Yokota A, Caro JF, Flier JS. 1989. Tissue-specific expression of two alternatively spliced insulin receptor mRNAs in man. Mol Endocrinol 3:1263–1269.

Moore MC, Smith MS, Sinha VP, Beals JM, Michael MD, Jacober SJ, Cherrington AD. 2014. Novel PEGylated basal insulin LY2605541 has a preferential hepatic effect on glucose metabolism. Diabetes 63:494–504.

Mosthaf L, Grako K, Dull TJ, Coussens L, Ullrich A, McClain DA. 1990. Functionally distinct insulin receptors generated by tissue-specific alternative splicing. EMBO J 9:2409–2413.

Owen OE, Morgan AP, Kemp HG, Sullivan JM, Herrera MG, Cahill GF, Jr. 1967. Brain metabolism during fasting. J Clin Invest 46:1589–1595.

Randle PJ, Garland PB, Newsholme EA, Hales CN. 1965. The glucose fatty acid cycle in obesity and maturity onset diabetes mellitus. Ann N Y Acad Sci 131:324–333.

Rizza RA, Mandarino LJ, Gerich JE. 1981. Dose-response characteristics for effects of insulin on production and utilization of glucose in man. Am J Physiol 240:E630–639.

Serrano R, Villar M, Martinez C, Carrascosa JM, Gallardo N, Andres A. 2005. Differential gene expression of insulin receptor isoforms A and B and insulin receptor substrates 1, 2 and 3 in rat tissues: Modulation by aging and differentiation in rat adipose tissue. J Mol Endocrinol 34:153–161.

Sesti G, Tullio AN, D'Alfonso R, Napolitano ML, Marini MA, Borboni P, Longhi R, Albonici L, Fusco A, Agliano AM, et al. 1994. Tissue-specific expression of two alternatively spliced isoforms of the human insulin receptor protein. Acta Diabetol 31:59–65.

Shojaee-Moradie F, Powrie JK, Sundermann E, Spring MW, Schuttler A, Sonksen PH, Brandenburg D, Jones RH. 2000. Novel hepatoselective insulin analog: Studies with a covalently linked thyroxyl-insulin complex in humans. Diabetes Care 23:1124–1129.

Sindelar DK, Balcom JH, Chu CA, Neal DW, Cherrington AD. 1996. A comparison of the effects of selective increases in peripheral or portal insulin on hepatic glucose production in the conscious dog. Diabetes 45:1594–1604.

Sindelar DK, Chu CA, Venson P, Donahue EP, Neal DW, Cherrington AD. 1998. Basal hepatic glucose production is regulated by the portal vein insulin concentration. Diabetes 47:523–529.

Stanley WC, Recchia FA, Lopaschuk GD. 2005. Myocardial substrate metabolism in the normal and failing heart. Physiol Rev 85:1093–1129.

Steil GM, Rebrin K, Mittelman SD, Bergman RN. 1998. Role of portal insulin delivery in the disappearance of intravenous glucose and assessment of insulin sensitivity. Diabetes 47:714–720.

Taniguchi CM, Emanuelli B, Kahn CR. 2006. Critical nodes in signalling pathways: Insights into insulin action. Nat Rev Mol Cell Biol 7:85–96.

Unger RH, Cherrington AD. 2012. Glucagonocentric restructuring of diabetes: A pathophysiologic and therapeutic makeover. J Clin Invest 122:4–12.

Ussar S, Vienberg SG, Kahn CR. 2011. Receptor antibodies as novel therapeutics for diabetes. Sci Transl Med 3:113ps47.

Vugmeyster Y, DeFranco D, Szklut P, Wang Q, Xu X. 2010. Biodistribution of [125I]-labeled therapeutic proteins: Application in protein drug development beyond oncology. J Pharm Sci 99:1028–1045.

Wang W, Wang EQ, Balthasar JP. 2008. Monoclonal antibody pharmacokinetics and pharmacodynamics. Clin Pharmacol Ther 84:548–558.

Yamaguchi Y, Flier JS, Yokota A, Benecke H, Backer JM, Moller DE. 1991. Functional properties of two naturally occurring isoforms of the human insulin receptor in Chinese hamster ovary cells. Endocrinology 129: 2058–2066.

Yip V, Palma E, Tesar DB, Mundo EE, Bumbaca D, Torres EK, Reyes NA, Shen BQ, Fielder PJ, Prabhu S, Khawli LA, Boswell CA. 2014. Quantitative cumulative biodistribution of antibodies in mice: Effect of modulating binding affinity to the neonatal Fc receptor. MAbs 6(3):689–96.

Zammit VA. 1996. Role of insulin in hepatic fatty acid partitioning: Emerging concepts. Biochem J 314(Pt 1):1–14.